A MODIFIED FINITE VOLUME APPROXIMATION OF SECOND-ORDER ELLIPTIC EQUATIONS WITH DISCONTINUOUS COEFFICIENTS *

R. EWING[†], O. ILIEV [‡], AND R. LAZAROV[§]

Abstract. A modified finite difference approximation for interface problems in R^n, $n = 1, 2, 3$ is presented. The essence of the modification falls in the simultaneous discretization of any two normal components of the flux at the opposite faces of the finite volume. In this way, the continuous normal component of the flux through an interface, is approximated by finite differences with second-order consistency. The derived scheme has a minimal $(2n + 1)$-point stencil for problems in R^n. Second-order convergence with respect to the discrete H^1-norm is proved for a class of interface problems. Second-order point-wise convergence is observed in a series of numerical experiments with 1-D, 2-D and 3-D interface problems. The numerical experiments presented demonstrate advantages of the new scheme compared with the known schemes which use arithmetic and harmonic averaging of the discontinuous diffusion coefficient.

Key words. finite volume method, interface problems, finite differences, elliptic problems with variable coefficients

AMS subject classifications. 65N10, 65F30

1. Introduction. Elliptic problems with discontinuous coefficients (often called interface problems) arise naturally in mathematical modeling processes in heat and mass transfer, diffusion in composite media, flows in porous media, etc. These processes are described by the model diffusion equation

$$(1.1) \qquad -\nabla(K\nabla u) = f(x) \text{ for } x \in \Omega,$$

subject to various boundary conditions. Here $\Omega \subset R^n$ is a bounded polyhedra, $K(x)$ is a symmetric and uniformly positive definite matrix in Ω which may have a jump discontinuity across a given surface Γ. Due to the nature of the processes, often the fluxes across Γ, defined as $-K\nabla u \cdot \mathbf{n}$, where $\mathbf{n}$ is the normal unit vector to Γ, are smooth, although the coefficients and the derivatives of the solution are discontinuous. Often the surfaces of discontinuity of the coefficient matrix $K(x)$ are called interfaces. The assumption that the solution and the normal component of the flux are continuous through the interface, is physical and is often used to close the mathematical problem. In this paper we derive a new class of finite difference schemes for second-order elliptic equations with diagonal coefficient matrix $K(x) = diag(k_1(x), \cdots, k_n(x))$. The derived schemes are based on finite volume techniques and use two main assumptions; (1) both the right hand side $f(x)$ and the normal components of the flux across the interface are smooth enough; (2) the interfaces Γ (i.e. the surfaces where the coefficients $k_i(x)$ have jumps) are parallel to the grid planes (lines).

In the one-dimensional case, the first assumption reduces just to the smoothness of the right hand side $f(x)$. In the multidimensional case, these two assumptions are much more complicated and restrictive. First, the interfaces have to be planes parallel to the coordinate planes. Second, the smoothness properties of the solution will depend on the smoothness of the boundary of the domain, the smoothness of the interface Γ, and on the ratio of the coefficient jumps in a pretty complicated manner. Some particular results in this direction can be found in the fundamental work of Kondratiev [12]. In general, when the normal component of the flux is smooth it makes sense to use schemes with better approximation properties away from the corners and the points of intersection of the interface Γ with itself or with the boundary $\partial\Omega$.

Finite difference schemes obtained from discretization of the balance equation over a finite number of control volumes have been widely used in computational practice for differential equations. In the early stages, these were finite difference schemes on rectangular meshes with quite complicated treatment of the coefficients and the right hand side (see, for example the classical books, [15, 17], and references therein). In [22, 23] Tikhonov and Samarskii derived an $O(h^{2m+1})$-accurate finite difference scheme, where $m \geq 0$ is an arbitrary integer, for two-point boundary value problems. The coefficients of the scheme are certain, in general, nonlinear functionals of the differential equation coefficients, which were assumed to be piece-wise smooth.

Further, in [20] Shashkov has extended the balance equation approximation idea to a large class of differential operators (including divergence, gradient, and curl) on quite general quadrilateral grids (see, also [7]). This new approach has produced discrete operators which approximate the corresponding differential operators and have the same properties as the continuous ones. For example, the discrete gradient is adjoint in a special inner product to the discrete divergence.

In recent years, the finite volume approach has been combined with finite element method techniques in a new development which is capable of producing accurate approximations on general triangular and quadrilateral grids (see, e.g. [2, 3, 4, 11, 13, 16]). The main advantages of the method are compactness of the discretization stencil, good accuracy, and local discrete conservation. In all of these discretization methods, it is assumed that the possible jumps of the diffusion coefficient are aligned with the finite element partitioning. This means, that inside each finite element the diffusion coefficient is sufficiently smooth and the jumps may occur only at the finite element boundaries.

A straightforward application of the finite volume method to a generic interface problem results in a scheme which uses harmonic averaging of the coefficient. This is particularly important in the case of discontinuous coefficients (see, for example, [17]). Inspecting these schemes, one easily sees that the normal component of the flux at the interface is discretized with a local truncation error $O(h)$. In this paper we present a modification of the classical finite volume method so the normal component of the flux in the new scheme has $O(h^2)$-local truncation for interface problems with smooth normal flux. Note, that we do not suppose that the interfaces are aligned with finite volume surfaces. However, we assume that the interfaces are orthogonal to the coordinate axes. Our approach can be viewed as a defect correction of the standard scheme with harmonic averaging of the coefficient, since it takes into account the next term in the Taylor expansion of the flux. This correction does preserve the standard $(2n + 1)$-point overall stencil and uses data only from the neighboring 2^n cells. We were able to increase the order of the local truncation error and at the same time to

preserve the standard stencil, by discretizing the normal components of the flux at the opposite sides of the finite volume as a couple.

Recently, Il'in [10] and LeVeque and Li [14] have derived second-order finite difference approximations of the 2-D interface problem using similar assumptions about the normal flux through the interface. However, in order to get a second-order scheme, Il'in uses a larger stencil than the compact $(2n+1)$-point stencils for problems in R^n, while LeVeque and Li [14] use Taylor expansions for the solution around the interface. The latter paper does not consider the discretization of the fluxes, and this can be viewed as a disadvantage when the problem requires their accurate reconstruction: for example velocities in porous media or the heat fluxes in thermal problems. Below we propose a homogeneous difference scheme for a class of 1-D, 2-D, and 3-D elliptic problems with variable discontinuous coefficients with arbitrarily located interfaces. The coefficients of the scheme are obtained from the coefficients of the differential equation by a simple formula. The approach of LeVeque and Li from [14] requires solving small systems of linear equations for determining these coefficients at each point near the interface. Moreover, our scheme is easily extendible to fine-scale inhomogeneities of the coefficients (finer than the grid size). However, our approach deals only with interfaces orthogonal to the coordinate axes, while the approach from [14] can treat arbitrarily located interfaces.

Below we summarize advantages and disadvantages of the new scheme in comparison with known ones for grids not aligned with the diffusion coefficient jump. On the positive side are the following features of the new scheme: (1) the scheme has $O(h^2)$-local truncation error for the normal component of the flux; recall that the standard schemes with arithmetic and harmonic averaging of the coefficient at the interface have in general local truncation error $O(1)$ and $O(h)$, respectively; (2) the proposed scheme is algebraically equivalent to a scheme which is second-order consistent to the interface differential problem; (3) the numerical experiments for problems with large jumps of the diffusion coefficient demonstrate that the new scheme is orders of magnitude more accurate than the scheme which uses harmonic averaging.

On the negative side are the following two main disadvantages: (1) in general, the scheme is only asymptotically (for $h \to 0$) locally conservative; (2) the corresponding matrix is a non-symmetric M-matrix; this will add some costs to the solution method for the algebraic problem. However, the numerical experiments on a wide class of problems with discontinuous coefficients show that the scheme is so accurate that these two disadvantages cannot diminish the value of the method.

We have run several numerical experiments in order to validate the new scheme, and to compare it with the known schemes. These experiments include solving 1-D, 2-D, and 3-D interface problems with known analytical solutions, as well as solving a 2-D problem with a singular solution. Also, we considered problems where the interfaces are aligned with the finite volume surfaces, as well as problems with arbitrarily located interfaces, orthogonal to the coordinate axes. Point-wise second-order convergence is observed in numerical experiments. Note, that the accuracy of the new scheme observed in our experiments is almost uniform with respect to the jump of coefficients, and it is comparable with the accuracy of the solution of the Poisson equation with constant diffusion coefficient. What is even more interesting is that this conclusion is valid not only for the case of interfaces aligned with the finite volume boundaries, but also for the non-aligned case. Meanwhile, for problems with large jumps of the coefficients, the accuracy of the scheme with harmonic averaging is very sensitive to the jump size and its accuracy is orders of magnitude less than the accuracy of the new

scheme. Numerical experiments for the so called thin lenses problem are especially interesting. In this case our scheme provides very accurate results even on very coarse grids, quite in contrast with the other known schemes.

The paper is organized as follows: Section 2 is devoted to the derivation and study of modified finite volume schemes for one-dimensional problems. Section 3 contains the formulation of the new finite volume scheme for multidimensional interface problems. Finally, Section 4 summarizes and discusses the results of the numerical experiments of a series on interface problems in R^n, $n = 1, 2, 3$.

2. Modified finite volume discretization for 1-D problems. In order to illustrate our approach we shall first consider the one-dimensional case and rewrite the equation (1.1) into its mixed form: find $u(x)$ such that

$$(2.1) \qquad \frac{\partial W}{\partial x} = f(x), \;\; W = -k(x)\frac{\partial u}{\partial x}, \;\; 0 < x < 1, \;\; u(0) = 0, \;\; u(1) = 0.$$

Here $k = k(x) > k_0$ is a known diffusion coefficient, $W(x)$ is the flux dependent variable, and $f(x)$ is the given source term. Conditions for continuity of the function and of the flux through interface points ξ are added:

$$(2.2) \qquad\qquad\qquad [u] = [W] = 0, \text{ for } x = \xi.$$

Here $[u]$ denotes the difference of the right and left limits of u at the point of discontinuity. The main assumptions for this problem are (1) the coeffcient $k(x)$ has a finite number of jump discontinuities and in the closed intervals between the jumps $k(x)$ is twice continuously differntiable; (2) the right hand side $f(x)$ is continuous and has continuous first derivative on the closed interval $[0, 1]$.

We introduce a standard uniform cell–centered grid $x_0 = 0, x_1 = h/2, x_i = x_{i-1} + h, i = 2, \cdots, N, x_{N+1} = 1$, where $h = 1/N$. Note, that the endpoints $x = 0$ and $x = 1$ are part of the grid, but they are at $h/2$ distance from their neighboring grid points. This type of shifted grid is slightly inconvenient for Dirichlet boundary conditions, but it is natural and very convenient for computations when the boundary condition involve the flux W. The internal grid points can be considered as centered around the volumes $V_i = (x_{i-\frac{1}{2}}, x_{i+\frac{1}{2}})$ where $x_{i+\frac{1}{2}} = x_i + \frac{1}{2}h, \; x_{i-\frac{1}{2}} = x_i - \frac{1}{2}h$. The values of a function f defined at the grid points x_i are denoted by f_i. Non-uniform grids can be treated in a similar way. A reason to work with cell-centred grids is that they are widely used, say, in the computational fluid dynamics. Considering, for example, non-isothermal fluid–structure interaction problems, one has to solve problems close to the one considered here. However, our approach is defined locally, at a particular finite volume level, and it can work with standard vertex-based grids, as well.

The finite volume method exploits the idea of writing the balance equation over the finite volume V_i, i.e. integrating the equation (2.1) over each volume V_i:

$$(2.3) \qquad W_{i+\frac{1}{2}} - W_{i-\frac{1}{2}} = h \, \varphi_i, \;\; \varphi_i = \frac{1}{h}\int_{x_{i-\frac{1}{2}}}^{x_{i+\frac{1}{2}}} f(x)dx, \;\; i = 1, 2, ..., N.$$

Next, we rewrite the flux equation in the form

$$-\frac{\partial u}{\partial x} = \frac{W(x)}{k(x)}$$

4

and integrate this expression over the interval (x_i, x_{i+1}):

$$(2.4) \qquad -(u_{i+1} - u_i) = -\int_{x_i}^{x_{i+1}} \frac{\partial u}{\partial x} dx = \int_{x_i}^{x_{i+1}} \frac{W(x)}{k(x)} dx.$$

We assume that flux $W(x)$ is two times continuously differentiable on the interface, so it can be expanded around the point $x_{i+\frac{1}{2}}$ in Taylor series

$$(2.5) \quad W(x) = W_{i+\frac{1}{2}} + (x - x_{i+\frac{1}{2}})\frac{\partial W_{i+\frac{1}{2}}}{\partial x} + \frac{(x - x_{i+\frac{1}{2}})^2}{2}\frac{\partial^2 W(\eta)}{\partial x^2}, \quad \eta \in (x_i, x_{i+1}).$$

After replacing the first derivative of the flux at $x_{i+\frac{1}{2}}$ by a two-point backward difference we get the following approximation of (2.4):

$$(2.6) \qquad -(u_{i+1} - u_i) = W_{i+\frac{1}{2}} \int_{x_i}^{x_{i+1}} \frac{dx}{k(x)}$$
$$+ \frac{W_{i+\frac{1}{2}} - W_{i-\frac{1}{2}}}{h} \int_{x_i}^{x_{i+1}} \frac{(x - x_{i+\frac{1}{2}})}{k(x)} dx + O(h^3).$$

Finally, we rewrite this equation in the following basic form:

$$(2.7) \qquad -k_{i+\frac{1}{2}}^H \frac{u_{i+1} - u_i}{h} = W_{i+\frac{1}{2}} + a_{i+\frac{1}{2}}(W_{i+\frac{1}{2}} - W_{i-\frac{1}{2}}) + \psi_i,$$

where

$$(2.8) \qquad k_{i+\frac{1}{2}}^H = \left(\frac{1}{h}\int_{x_i}^{x_{i+1}}\frac{dx}{k(x)}\right)^{-1},$$
$$a_{i+\frac{1}{2}} = k_{i+\frac{1}{2}}^H \frac{1}{h^2}\int_{x_i}^{x_{i+1}}\frac{x - x_{i+\frac{1}{2}}}{k(x)}dx, \quad \psi_i = O(h^2).$$

Here $k_{i+\frac{1}{2}}^H$ is the well known harmonic averaging of the coefficient $k(x)$ over the cell (x_i, x_{i+1}), which has played a fundamental role in deriving accurate schemes for discontinuous coefficients (see, e.g. [15, 17]). This presentation of the flux $W(x)$ is a starting point for our discretization. Since we have assumed that the flux is smooth, then the consecutive terms in the right hand side in (2.7) are $O(1)$, $O(h)$ and $O(h^2)$, respectively. Truncation of this sum after the first term produces the well known scheme of Samarskii [17] with harmonic averaging of the coefficient. This scheme is $O(h)$-consistent at the interface points and second-order accurate in the discrete H^1-norm. Further in the text we call this scheme *harmonic averaging* or HA scheme. The scheme we shall derive takes the two terms of the presentation (2.7), and disregards the ψ_i-term. Let $F_{i+\frac{1}{2}}$ and $F_{i-\frac{1}{2}}$ denote the approximation to the exact fluxes $W_{i+\frac{1}{2}}$ and $W_{i-\frac{1}{2}}$, respectively, and let y_i denote the approximate values of the exact solution $u(x_i)$. Thus, we get the following relations:

$$(2.9) \qquad -k_{i+\frac{1}{2}}^H \frac{y_{i+1} - y_i}{h} = F_{i+\frac{1}{2}} + a_{i+\frac{1}{2}}(F_{i+\frac{1}{2}} - F_{i-\frac{1}{2}}),$$

$$(2.10) \qquad -k_{i-\frac{1}{2}}^H \frac{y_i - y_{i-1}}{h} = F_{i-\frac{1}{2}} + a_{i-\frac{1}{2}}(F_{i+\frac{1}{2}} - F_{i-\frac{1}{2}}).$$

The above two relations allow us to derive the final expression for $F_{i+\frac{1}{2}} - F_{i-\frac{1}{2}}$, which is needed in the balance equation (2.3): subtract (2.10) from (2.9) to get

$$(2.11) \quad (1 + a_{i+\frac{1}{2}} - a_{i-\frac{1}{2}})(F_{i+\frac{1}{2}} - F_{i-\frac{1}{2}}) = -k_{i+\frac{1}{2}}^H \frac{y_{i+1} - y_i}{h} + k_{i-\frac{1}{2}}^H \frac{y_i - y_{i-1}}{h}.$$

Since the grid points x_0 and x_{N+1} are shifted by $h/2$ from their neighbors, the finite difference equations at x_1 and x_N have to be modified. Combining (2.11) with (2.3) we get the following finite difference approximation of the differential problem (2.1):

$$(2.12) \qquad\qquad L_h y_i = \varphi_i \quad \text{for} \quad i = 1, \cdots, N.$$

where

$$L_h y_i \equiv \begin{cases} -\dfrac{4}{3}\dfrac{1}{h}\left(k_{\frac{3}{2}}^H \dfrac{y_2 - y_1}{h} - k_{\frac{1}{2}}^H \dfrac{2y_1}{h}\right) (\text{ for } i = 1), \\[3mm] -\left(1 + a_{i+\frac{1}{2}} - a_{i-\frac{1}{2}}\right)^{-1}\dfrac{1}{h}\left(k_{i+\frac{1}{2}}^H \dfrac{y_{i+1} - y_i}{h} - k_{i-\frac{1}{2}}^H \dfrac{y_i - y_{i-1}}{h}\right), \ i \neq 1, N, \\[3mm] -\dfrac{4}{3}\dfrac{1}{h}\left(-k_{N+\frac{1}{2}}^H \dfrac{2y_N}{h} - k_{N-\frac{1}{2}}^H \dfrac{y_N - y_{N-1}}{h}\right) (\text{ for } i = N). \end{cases}$$

(2.13)

Here in the first and last difference equations, we have explicitly imposed the homogeneous boundary conditions $y_0 = 0$ and $y_{N+1} = 0$. Further in the text we refer to this approximation as a scheme using *improved harmonic averaging* or IHA scheme.

REMARK 2.1. *For $a_{i+\frac{1}{2}} = a_{i-\frac{1}{2}} = 0$, the operator L_h is the well known finite difference operator corresponding to harmonic averaging of the diffusion coefficient, which is second-order accurate in the discrete H^1-norm (see, e.g. [17]).*

REMARK 2.2. *Near the boundary the discretization (2.13) has a special form due to the use of a cell-centered grid. The well known discretization for such grids uses the factor 1 instead of $\frac{4}{3}$. Although the difference scheme with the factor 1 is not consistent with the differential problem at the points x_1, x_N, it is proven (see, for example, [25]) that this does not influence the order of convergence of the scheme. We prefer the factor $\frac{4}{3}$ because the fluxes at $x = 0$ and $x = 1$ are $O(h^2)$-accurate in this case. Moreover, the numerical experiments of numerous test problems with continuous and discontinuous coefficients showed that the constant in the convergence was smaller when the discretization (2.12)-(2.13) was used.*

REMARK 2.3. *Alternative ways for deriving 3-point approximations of one-dimensional problems in the framework of the finite element method are discussed, for example, in [5] and [24]. In the latter work the finite element spaces involve the local solutions of the problem (2.1), while in the former work the schemes are derived by the dual mixed hybrid formulation.*

In our computations for comparison of the performance of the new scheme, we also use the scheme (2.12) in which $a_{i+\frac{1}{2}} = a_{i-\frac{1}{2}} = 0$ and $k_{i+\frac{1}{2}}^H$ is replaced by $0.5(k_i + k_{i+1})$. This scheme is referred to as the *arithmetic averaging (AA)* scheme.

Accurate computations of the fluxes are needed in many applications. The following expression approximates the continuous flux with second-order accuracy (even at the interface):

$$(2.14) \qquad F_{i+\frac{1}{2}} = \frac{-k_{i+\frac{1}{2}}^H \frac{y_{i+1}-y_i}{h}\left(1 - a_{i-\frac{1}{2}}\right) - k_{i-\frac{1}{2}}^H \frac{y_i-y_{i-1}}{h}\left(a_{i+\frac{1}{2}}\right)}{\left(1 + a_{i+\frac{1}{2}}\right)\left(1 - a_{i-\frac{1}{2}}\right) + a_{i+\frac{1}{2}}a_{i-\frac{1}{2}}}$$

$$= W_{i+\frac{1}{2}} + O(h^2).$$

The new scheme approximates the fluxes to second-order accuracy, *independent* of the positions of the discontinuity of the coefficient $k(x)$. The price we paid is the necessity to evaluate the expressions $k^H_{i+\frac{1}{2}}$ and $a_{i+\frac{1}{2}} - a_{i-\frac{1}{2}}$ with an error no larger than $O(h^2)$. We shall assume that any point ξ where the coefficient $k(x)$ is discontinuous is known and can be presented in the form $\xi = x_i + \theta h$ for some i and $0 \leq \theta \leq 1$.

Obviously, if $\theta = 0$ or $\theta = 1$ (i.e., when the interfaces are aligned with grid nodes), then $a_{i+\frac{1}{2}} - a_{i-\frac{1}{2}} = O(h^2)$. Thus, disregarding this term and taking into account that $k^H_{i+\frac{1}{2}} = k(x_{i+\frac{1}{2}}) + O(h^2)$ we end up with a scheme which is the same as those obtained from finite difference or linear finite element approximations. Further, if the diffusion coefficient $k(x)$ has jump discontinuities and $0 < \theta < 1$, but the flux is still smooth, the second term in the right hand side in (2.6) will be essential to derive a better approximation. *Note, that accounting for this second term is the main difference between our approach and the standard finite volume discretization of interface problems.* In short, this term does not affect the order of convergence, but allows us to improve the constant of convergence in the case of discontinuous coefficients and to derive more accurate difference schemes.

Now we consider particular realizations of this scheme. If the point of discontinuity ξ is in the subinterval $[x_i, x_{i+1}]$: $\xi = x_i + \theta h$, where $0 \leq \theta \leq 1$, then the approximation of the integral in $k^H_{i+\frac{1}{2}}$ is done by splitting it into integrals over (x_i, ξ) and (ξ, x_{i+1}) and then applying the trapezoidal or midpoint rule for each integral. This approach will produce accurate enough evaluation of $k^H_{i+\frac{1}{2}}$. The following formula will be only $O(h)$-accurate:

$$k^H_{i+\frac{1}{2}} \approx \left(\frac{\theta}{k_i} + \frac{1-\theta}{k_{i+1}} \right)^{-1}.$$

Note that in the case of piece-wise constant coefficients, this formula is exact. However, it is based on the use of left and right rectangular quadrature formulae, and might not be accurate enough in the general case. Second-order accurate evaluation of the integrals is given by

$$(2.15) \qquad k^H_{i+\frac{1}{2}} \approx \left[\frac{\theta}{2} \left(\frac{1}{k_i} + \frac{1}{k_{\xi-0}} \right) + \frac{1-\theta}{2} \left(\frac{1}{k_{i+1}} + \frac{1}{k_{\xi+0}} \right) \right]^{-1}.$$

Note, that $k_{\xi-0}, k_{\xi+0}$ are known from the second interface condition (2.2).

Further, we continue with the second integral in (2.8). Our aim is to obtain a second-order approximation for the flux $W(x)$. We again split the integral into two integrals and apply the trapezoidal rule for each of the two integrals:

$$\frac{1}{h^2} \int_{x_i}^{x_{i+1}} \frac{(x - x_{i+1})}{k(x)} dx = \frac{1}{h^2} \int_{x_i}^{\xi} \frac{(x - x_{i+\frac{1}{2}})}{k(x)} dx + \frac{1}{h^2} \int_{\xi}^{x_{i+1}} \frac{(x - x_{i+\frac{1}{2}})}{k(x)} dx =$$

$$(2.16) \quad = \frac{\theta}{2} \left(\frac{\theta - 0.5}{k_{\xi-0}} - \frac{0.5}{k_i} \right) + \frac{1-\theta}{2} \left(\frac{0.5}{k_{i+1}} + \frac{\theta - 0.5}{k_{\xi+0}} \right) + O(h^2).$$

The case of piece-wise constant coefficient $k(x)$ is very important for the applications. In this case the formulas presented above are exact and reduce to

$$(2.17) \qquad k^H_{i+\frac{1}{2}} = \left(\frac{\theta}{k_i} + \frac{1-\theta}{k_{i+1}} \right)^{-1} \quad \text{and} \quad a_{i+\frac{1}{2}} = \frac{1}{2} \frac{\theta(1-\theta)(k_i - k_{i+1})}{(1-\theta)k_i + \theta k_{i+1}}.$$

Obviously, if the point of discontinuity ξ is a midpoint of the grid, i.e. $\xi = x_{i+\frac{1}{2}}$, then $\theta = 1/2$ and

$$k_{i+\frac{1}{2}}^H = 2\left(\frac{1}{k_i} + \frac{1}{k_{i+1}}\right)^{-1} \quad \text{and } a_{i+\frac{1}{2}} = \frac{1}{4}\left(\frac{k_i - k_{i+1}}{k_i + k_{i+1}}\right).$$

It is reasonable to assume that the step size h is so small, that if there is a jump in the coefficient $k(x)$ in the interval (x_i, x_{i+1}), then $k(x)$ is smooth at the neighboring two intervals (x_{i-1}, x_i) and (x_{i+1}, x_{i+2}). Thus,

$$1 + a_{i+\frac{1}{2}} - a_{i-\frac{1}{2}} = 1 + \frac{\theta(1-\theta)}{2}\left(\frac{k_i - k_{i+1}}{(1-\theta)k_i + \theta k_{i+1}}\right) + O(h^2) \geq 1/2.$$

Similarly, we also have an estimate from above: $1 + a_{i+\frac{1}{2}} - a_{i-\frac{1}{2}} \leq 3/2$. These two estimates will guarantee that the finite difference scheme is well conditioned.

The following result is valid:

PROPOSITION 1. *Assume that the coefficient $k(x)$ is a piecewise C^1-function and has a finite number of jump discontinuities, the grid is such that the discontinuities are at the points $x_{i+\frac{1}{2}}$, and the source term $f(x)$ is a C^1-function on $(0,1)$. Then the finite difference scheme (2.12), (2.8), (2.15), (2.16) is second-order accurate in the discrete H^1-norm, i.e. the error $e_i = u(x_i) - y_i$ satisfies the estimate*

$$\|e\|_{H^1} \equiv \|y - u\|_{H^1} \equiv \left(\sum_{i=1}^{N} k_{i-1/2}^H (e_i - e_{i-1})^2 / h\right)^{1/2} \leq M\, h^2.$$

The second-order of accuracy in H^1 follows from the second-order of discretization for the fluxes by using the classical technique for deriving *a priori* estimates for the solution of the finite difference scheme (see, e.g. [17, 18]).

REMARK 2.4. *Note that if $f(x) \equiv 1$ then $W''(x) \equiv 0$ and the local truncation error is identically zero. This means that the IHA scheme is exact (i.e., it reproduces exactly the solution at the grid points) for problems with piecewise constant diffusion coefficient and constant right hand side, while the HA scheme is exact only for homogeneous problems. Thus, HA scheme reproduces exactly piecewise linear solutions, while the IHA scheme reproduces exactly piecewise quadratic solutions.*

3. Modified finite volume discretization for 3-D problems. In this section we shall introduce the finite difference scheme for the equation (1.1) in R^3 with homogeneous Dirichlet boundary conditions on a rectangular domain Ω. Now we introduce the flux $\mathbf{W} = -K(x)\nabla u$. If the diffusion coefficient is discontinuous on a certain surface (so-called interface denoted by Γ), then two conditions for continuity of the solution and the normal component of the flux through the interface are added:

(3.1) $$[u] = 0, \quad [\mathbf{W} \cdot \mathbf{n}] = 0, \quad x \in \Gamma,$$

where $[g]$ denotes the difference of the limit values of the function g from both sides of Γ and $\mathbf{n}$ is the unit vector normal to Γ.

In this paper we consider multidimensional problems that can be discretized in a coordinate-wise way. This means that the interfaces are parallel to the faces of the finite volumes and the diffusion coefficient matrix $K(x)$ is a diagonal. Thus, the discretization of a 3-D problem is obtained as a tensor product discretization of three 1-D problems (like one investigated in the preceding section).

The finite volume approach is used for discretizing the above equation on cell-centered grids which are tensor products of grids in each direction. The grid sizes and the number of the nodes in the x_i-direction is h_i and N_i, for $i = 1, 2, 3$. The grid points are denoted by $(x_{1,i}, x_{2,j}, x_{3,k})$, where $0 \le i \le N_1$, $0 \le j \le N_2$, $0 \le k \le N_3$. The values of the unknown function are related to the volumes' centers. The discretization at the internal points is based on the local flux balance for the finite volume around the point. For the finite volume V_P corresponding to node P this balance is:

$$(3.2) \qquad \int_{\partial V_P} \mathbf{W} \cdot \mathbf{n} ds = h_1 h_2 h_3 \varphi_P, \quad \varphi_P = \frac{1}{h_1 h_2 h_3} \int_{V_P} f(x) dx.$$

Here $\mathbf{n}$ is the unit outward normal to the volume boundary ∂V_P. Next, we approximate the integrals over the volume faces by the midpoint rule to get

$$\begin{aligned} h_2 h_3 \left(W_e - W_w \right) & + h_3 h_1 \left(W_n - W_s \right) \\ (3.3) \qquad & + h_1 h_2 \left(W_t - W_b \right) = h_1 h_2 h_3 \varphi_P + O(h^2). \end{aligned}$$

Subscripts with capital letters W, E, S, N, B, T are used to denote the values at the west, east, south, north, bottom and top neighboring grid points and the subscript P is used for the center of the stencil, while w, e, s, n, b, t stand for the respective values in the center points of the control volume faces. For example, $W_e = -k_1 \frac{\partial u}{\partial x_1}|_{x_e}$ is the flux through a face perpendicular to the axis x_1 at the point $x_e = (x_{1,i+\frac{1}{2}}, x_{2,j}, x_{3,k})$, the grid point P is denoted by $x_P = (x_{1,i}, x_{2,j}, x_{3,k})$. The grid point east of P is denoted by $x_E = (x_{1,i+1}, x_{2,j}, x_{3,k})$, while that north of P is $x_N = (x_{1,i}, x_{2,j+1}, x_{3,k})$, etc. Further, we approximate the differences $W_e - W_w$, $W_n - W_s$, and $W_t - W_b$ as one-dimensional fluxes in the directions x_1, x_2, and x_3, correspondingly, using formula (2.11) in each direction.

In the particular case when the diffusion coefficient is a constant within any finite volume and the interfaces are aligned with finite volume surfaces (i.e. $\theta = 0.5$), the finite volume scheme, approximating the 3-D problem and preserving second-order of discretization for the normal components of the fluxes through interfaces, can be written as

$$\begin{aligned} h_2 h_3 \mu_1^{-1} \left[k_e^H \frac{y_E - y_P}{h_1} - k_w^H \frac{y_P - y_W}{h_1} \right] & + h_3 h_1 \mu_2^{-1} \left[k_n^H \frac{y_N - y_P}{h_2} - k_s^H \frac{y_P - y_S}{h_2} \right] + \\ (3.4) \qquad & + h_1 h_2 \mu_3^{-1} \left[k_u^H \frac{y_T - y_P}{h_3} - k_d^H \frac{y_P - y_B}{h_3} \right] = h_1 h_2 h_3 \varphi_P, \end{aligned}$$

where

$$\mu_1 = \left[1 + \frac{1}{4} \left(\frac{k_{1,P} - k_{1,E}}{k_{1,P} + k_{1,E}} + \frac{k_{1,P} - k_{1,W}}{k_{1,P} + k_{1,W}} \right) \right],$$

$$\mu_2 = \left[1 + \frac{1}{4} \left(\frac{k_{2,P} - k_{2,N}}{k_{2,P} + k_{2,N}} + \frac{k_{2,P} - k_{2,S}}{k_{2,P} + k_{2,S}} \right) \right],$$

$$\mu_3 = \left[1 + \frac{1}{4} \left(\frac{k_{3,P} - k_{3,T}}{k_{3,P} + k_{3,T}} + \frac{k_{3,P} - k_{3,B}}{k_{3,P} + k_{3,B}} \right) \right].$$

Here k_e^H stands for harmonic averaging of $k_1(x)$ in direction east from P, i.e. over the interval $(x_{1,i}, x_{1,i+1})$, $k_{1,P}$ is its value at the point P, etc. These finite difference

equations are written for all internal points except those for which the $(2n+1)$-stencil includes points at the boundary. For these points essentially one has to add the modification of the approximation at the direction of the neighboring boundary point. Such modification has been introduced for one-dimensional problems in Section 2 (see formulas (2.12) - (2.13)). To close the system to this set of finite difference equations we add the equations accounting for the Dirichlet boundary conditions.

Note, that in the case when the interfaces are not aligned with the finite volume surfaces (but are orthogonal to the axes), the multidimensional θ-HA scheme, as well as the multidimensional θ-IHA scheme, are derived as tensor products of the respective one-dimensional schemes.

It is obvious that the finite difference scheme can be written as a linear system of algebraic equations with a non-symmetric M-matrix. If the coefficients $k_i(x)$, $i = 1, \cdots, n$ are C^2-functions in the whole domain, then the factors μ_1, μ_2, and μ_3 are all of the order $O(h^2)$ and the non-symmetry is negligible. On the other hand, $\mu_i > 1/2$, $i = 1, 2, 3$ for grids with jump discontinuities of the coefficient $k_i(x)$ parallel to the grid faces, regardless of the size and of the jump. Therefore, although the condition number of the linear system will depend on the size of the jump, this dependence will be the same as in the case of arithmetic or harmonic averaging. The finite difference scheme (3.4) is the IHA scheme that has been used in our numerical experiments for both two-dimensional and three-dimensional problems, in the case when the interfaces are aligned with the finite volume surfaces. The multidimensional θ-HA scheme and θ-IHA scheme are used in the non-aligned case.

4. Numerical Experiments. A series of computational experiments were performed in order to experimentally study the accuracy and the convergence rate of the new scheme and to compare it with known schemes for 1-D, 2-D and 3-D interface problems. Two kind of problems were solved in 1-D and 2-D cases. The first one is a problem with known analytical solution with the right hand side being calculated from the known solution. The second one is a problem with right hand side identically equal to 1. Note that in the 1-D case this problem also has an analytical solution. Only problems with known analytical solutions are solved in the 3-D case.

Relative discrete maximum norm (denoted as C-norm) of the solution error (i.e. of the difference between the exact and the computed solution) is calculated as $\max |u - y| / \max |u|$. Also, the relative discrete L_2-norm of the solution error is computed as $\left(\sum_V meas(V)(u - y)^2 \right)^{\frac{1}{2}} / \max |u|$. Here the operations max and the summation are considered over all grid nodes. The relative C- and L_2-norms of the error are reported in the tables below for cases when the analytical solution is known. In all tables we have used the following shorthand notations: B stands for the problem when $k(x) \equiv 1$, i.e. we solve the Poisson equation, AA - for schemes with arithmetic averaging, HA - for schemes with harmonic averaging, and finally, IHA is used for a heading the results obtained by the new scheme which uses improved harmonic averaging.

4.1. Numerical experiments for 1-D problems. Results from the problem computation with exact solution $u^{ex} = \frac{1}{k} sin \left(\frac{\pi x}{2} \right) \left(x - \frac{1}{2} \right) \left(1 + x^2 \right)$ and diffusion coefficient equal to 1 for $0 < x < 0.5$ and equal to 10^{-4} for $0.5 < x < 1$ are presented in Tables 4.1 and 4.2 below.

Results from solving the Dirichlet problem with right hand side identically equal to 1 are presented in Tables 4.3 and 4.4. Diffusion coefficient in this case is 1 for $0 < x < 0.4$, 10^{-3} for $0.4 < x < 0.7$, and 10 for $0.7 < x < 1$. Note, that this problem has a piecewise quadratic solution.

TABLE 4.1

1-D problem with $u^{ex} = \frac{1}{k}\sin\left(\frac{\pi x}{2}\right)\left(x - \frac{1}{2}\right)\left(1 + x^2\right)$; $k = \{1, 10^{-4}\}$ *in 2 subregions, respectively; the relative C-norms of the error and their ratios*

Nodes	$k = \{1, 10^{-4}\}$					
	case AA		case HA		case IHA	
12	4.95d-2	–	4.49d-3	–	5.41d-4	–
22	2.34d-2	2.12	1.28d-3	3.51	1.98d-4	2.73
42	1.13d-2	2.07	3.24d-4	3.95	5.90d-5	3.35
82	5.60d-3	2.02	8.14d-5	3.98	1.60d-5	3.69
162	2.78d-3	2.01	2.04d-5	3.99	4.17d-6	3.84

TABLE 4.2

1-D problem with $u^{ex} = \frac{1}{k}\sin\left(\frac{\pi x}{2}\right)\left(x - \frac{1}{2}\right)\left(1 + x^2\right)$; $k = \{1, 10^{-4}\}$ *in 2 subregions, respectively; the relative L_2-norms of the error and their ratios*

Nodes	$k = \{1, 10^{-4}\}$					
	case AA		case HA		case IHA	
12	2.25d-2	–	2.39d-3	–	2.58d-4	–
22	1.01d-2	2.23	6.20d-4	3.85	9.50d-5	2.72
42	4.78d-3	2.11	1.58d-4	3.92	2.91d-5	3.26
82	2.32d-3	2.06	4.00d-5	3.95	8.02d-6	3.63
162	1.14d-3	2.04	1.00d-5	4.00	2.10d-6	3.82

The results from numerical experiments in 1-D case demonstrate that the new scheme has a much smaller constant of convergence than the scheme based on harmonic averaging. Both schemes asymptotically converge with second-order, as predicted by the theory. The Tables 4.3 and 4.4 confirm the theory that IHA scheme is exact for interface problems with piecewise quadratic solution.

4.2. Numerical experiments for 2-D problems. Here we consider an isotropic case, i.e. $k_i(x) = k(x)$, $i = 1, \cdots, n$. First of all, a two-dimensional interface problem with different coefficient in 4 subregions and with a known analytical solution is solved. We compute the solution using schemes obtained from harmonic (HA), and improved harmonic (IHA) averaging of the diffusion coefficient. Notations HA and IHA are preserved for the case when $\theta = \frac{1}{2}$, while notations θ-HA and θ-IHA are used for other values of θ. Two sets of values for the diffusion coefficient in the 4 subregions, are used in order to demonstrate the influence of the size of the jump discontinuity on the accuracy of the schemes. Results from these computations are presented in Tables 4.5 and 4.2 for the first set, and in Tables 4.7 and 4.8 for the second set.

Let us discuss the results presented in Tables $4.5 - 4.8$. The scheme with harmonic averaging of $k(x)$ is $O(h^2)$-accurate. The new scheme also converges with second-order, but the constant in front of the convergence factor is two orders of magnitude smaller for the example with large jumps of the coefficients. This means that in practical computations the new scheme allows computations on significantly coarser grids in comparison with known schemes. The accuracy of the new scheme is almost uniform with respect to the size of the jump discontinuity, as one can observe from the Tables, and it is comparable with the accuracy of computing the Poisson equation with a constant coefficient (denoted as case B in the Tables). An interesting fact is that the IHA scheme preserves this behavior even in the case when interfaces are not aligned with the finite volume boundaries. At the same time the accuracy of the HA scheme depends on the jump discontinuity. Note, that the larger the jump of the coefficient, the better the advantages of the IHA scheme are seen.

The results in the non-aligned case need special discussion. It was observed in

TABLE 4.3
1-D problem $-(ku')' = 1, u(0) = 0, u(1) = 1$; $k = \{1, 10^{-3}, 10\}$ *in 2 subregions, respectively; the relative C-norms of the error and their ratios*

Nodes	$k = \{1, 10^{-3}, 10\}$					
	case AA		case HA		case IHA	
12	5.39d-1	–	1.06d-1	–	3.6d-15	*exact*
22	3.02d-1	1.78	2.70d-2	3.93	3.3d-15	*exact*
42	1.55d-1	1.95	6.63d-3	4.07	5.1d-15	*exact*
82	7.89d-2	1.96	1.65d-3	4.02	5.3d-15	*exact*
162	3.98d-2	1.98	4.13d-4	3.99	1.0d-14	*exact*

exact ≡ the difference scheme is exact for this problem.

TABLE 4.4
1-D problem $-(ku')' = 1, u(0) = 0, u(1) = 1$; $k = \{1, 10^{-3}, 10\}$ *in 3 subregions, respectively; the relative L_2-norms of the error and their ratios*

Nodes	$k = \{1, 10^{-3}, 10\}$					
	case AA		case HA		case IHA	
12	2.89d-1	–	5.79d-2	–	1.3d-15	*exact*
22	1.62d-1	1.78	1.48d-2	3.91	1.4d-15	*exact*
42	8.34d-2	1.94	3.63d-3	4.08	1.1d-15	*exact*
82	4.24d-2	1.97	9.04d-4	4.02	1.2d-15	*exact*
162	2.14d-2	1.98	2.26d-4	4.00	2.7d-15	*exact*

exact≡the difference scheme is exact for this problem.

TABLE 4.5
2-D problem with $u^{ex} = \frac{1}{k} sin\left(\frac{\pi x}{2}\right)\left(x - x_\xi\right)\left(y - y_\xi\right)\left(1 + x^2 + y^2\right)$ *and* $k = \{10^{-2}, 1, 10^{-4}, 10^{+6}\}$ *in 4 subregions with interfaces at* $x = x_\xi$ *and* $y = y_\xi$; *the relative C-norms of the error and their ratios*

Grid	$k(x,y) \equiv 1$		$x_\xi = \frac{1}{2}, y_\xi = \frac{1}{2}$, (aligned)				$x_\xi = \frac{1}{3}, y_\xi = \frac{1}{3}$, (non-aligned)			
	case B		HA scheme		IHA scheme		θ-HA scheme		θ-IHA scheme	
12x12	2.09d-4	–	1.75d-4	–	3.34d-4	–	1.91d-2	–	4.48d-4	–
22x22	5.74d-5	3.6	5.97d-3	2.9	7.64d-5	4.4	9.56d-3	2.0	1.45d-4	3.1
42x42	1.75d-5	3.7	1.80d-3	3.3	1.94d-5	3.9	2.10d-3	4.6	4.02d-5	3.6
82x82	4.11d-6	3.8	5.03d-4	3.6	4.97d-6	3.9	7.03d-4	3.0	1.10d-5	3.7
162x162	1.06d-6	3.9	1.36d-4	3.7	1.26d-6	3.9	1.64d-4	4.3	2.80d-6	3.9

TABLE 4.6
2-D problem with $u^{ex} = \frac{1}{k} sin\left(\frac{\pi x}{2}\right)\left(x - x_\xi\right)\left(y - y_\xi\right)\left(1 + x^2 + y^2\right)$ *and* $k = \{10^{-2}, 1, 10^{-4}, 10^{+6}\}$ *in 4 subregions with interfaces at* $x = x_\xi$ *and* $y = y_\xi$; *the relative L_2-norms of the error and their ratios*

Grid	$k(x,y) \equiv 1$		$x_\xi = \frac{1}{2}, y_\xi = \frac{1}{2}$, (aligned)				$x_\xi = \frac{1}{3}, y_\xi = \frac{1}{3}$, (non-aligned)			
	case B		HA scheme		IHA scheme		θ-HA scheme		θ-IHA scheme	
12x12	7.79d-5	–	2.80d-3	–	8.05d-5	–	3.66d-3	–	9.72d-5	–
22x22	2.16d-5	3.6	7.98d-4	3.5	1.71d-5	4.7	1.41d-4	2.6	3.50d-5	2.8
42x42	5.93d-6	3.6	2.09d-4	3.8	4.30d-6	4.0	2.90d-4	4.9	9.48d-6	3.7
82x82	1.58d-6	3.8	5.34d-5	3.9	1.12d-6	3.8	8.12d-5	3.6	2.66d-6	3.6
162x162	4.09d-7	3.9	1.35d-5	4.0	2.87d-7	3.9	1.92d-5	4.2	6.82d-7	3.9

TABLE 4.7
2-D problem with $u^{ex} = \frac{1}{k} sin\left(\frac{\pi x}{2}\right)\left(x - x_\xi\right)\left(y - y_\xi\right)\left(1 + x^2 + y^2\right)$ *and* $k = \{10, 10^{-1}, 10^3, 1\}$ *in 4 subregions with interfaces at* $x = x_\xi$ *and* $y = y_\xi$; *the relative C-norms of the error and their ratios*

Grid	$k(x,y) \equiv 1$		$x_\xi = \frac{1}{2}, y_\xi = \frac{1}{2}$, (aligned)				$x_\xi = \frac{1}{3}, y_\xi = \frac{1}{3}$, (non-aligned)			
	case B		HA scheme		IHA scheme		θ-HA scheme		θ-IHA scheme	
12x12	2.09d-4	–	2.32d-3	–	2.32d-4	–	8.47d-4	–	2.84d-4	–
22x22	5.74d-5	3.6	7.72d-4	3.0	6.88d-5	3.4	2.14d-4	4.0	6.20d-5	4.6
42x42	1.75d-5	3.7	2.33d-4	3.3	1.92d-5	3.6	8.98d-5	2.4	1.10d-5	5.6
82x82	4.11d-6	3.8	6.50d-5	3.6	5.09d-6	3.8	2.08d-5	4.3	4.30d-6	2.6
162x162	1.06d-6	3.9	1.74d-5	3.7	1.31d-6	3.9	6.60d-6	3.2	6.40d-7	6.7

TABLE 4.8

2-D problem with $u^{ex} = \frac{1}{k}\sin\left(\frac{\pi x}{2}\right)\left(x - x_\xi\right)\left(y - y_\xi\right)\left(1 + x^2 + y^2\right)$ and $k = \{10, 10^{-1}, 10^3, 1\}$ in 4 subregions with interfaces at $x = x_\xi$ and $y = y_\xi$; the relative L_2-norm of the error and their ratios

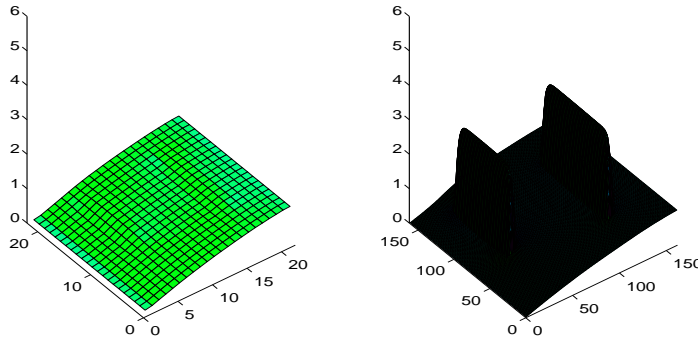| Grid	$k(x,y) \equiv 1$ case B		$x_\xi = \frac{1}{2}, y_\xi = \frac{1}{2}$, (aligned) HA scheme		IHA scheme		$x_\xi = \frac{1}{3}, y_\xi = \frac{1}{3}$, (non-aligned) θ-HA scheme		θ-IHA scheme	
12x12	7.79d-5	–	4.11d-4	–	6.18d-5	–	1.70d-4	–	6.37d-5	–
22x22	2.16d-5	3.6	1.20d-4	3.4	1.65d-5	3.8	4.30d-5	4.0	1.99d-5	3.2
42x42	5.93d-6	3.6	3.31d-5	3.6	4.75d-6	3.5	1.14d-5	3.8	3.32d-6	6.0
82x82	1.58d-6	3.8	8.34d-6	4.0	1.26d-6	3.8	2.84d-6	4.0	1.25d-6	2.7
162x162	4.09d-7	3.9	2.11d-6	4.0	3.31d-7	3.8	7.24d-7	3.9	2.10d-7	6.0

FIG. 4.1. *Graph of 2-D thin lenses computations with the AA scheme; left: grid 22×22, right: grid 162×162*

the experiments, that the θ-schemes converge uniformly (with respect to refinement of the grid) with second-order, only if the grid is refined in a such a way, that θ remains constant. In our experiments θ varies from one grid to the next, and this is the reason for the non-monotone values obtained for the ratios of the norms of the error on consecutive grids. A possible explanation of such a behavior is that the reminder term is different for the cases $0 \leq \theta \leq 0.5$ and $0.5 \leq \theta \leq 1$. This phenomena needs further detailed investigations.

As a second 2-D example, an interface problem with right hand side identically equal to one is considered. Dirichlet boundary conditions on the east and west sides and zero Neumann boundary conditions on the north and south sides are prescribed. The computed problem is also known as a thin lenses problem: the diffusion coefficient is very small within two thin lenses, and is equal to 1 elsewhere. In our computations the lenses are $\{0.4 < x_1 < 0.9; \ 0.2 < x_2 < 0.25\}$ and $\{0.2 < x_1 < 0.8; \ 0.7 < x_2 < 0.75\}$. The diffusion coefficient of the lenses has value 10^{-4}. The analytical solution of the problem is not known. The solution of the problem has singularities around corners of the lenses, and $u \in W_2^{1+\beta}$, where $\beta \sim \frac{1}{3}$ for our examples (for details see [21]). The computed solutions are presented in Figure 4.2 for the AA scheme, in Figure 4.2 for the HA scheme, and in Figure 4.2 for the IHA scheme. The left plot on any figure presents the solution on a coarse 22×22 grid, while the right plot presents the solution on a fine 162×162 grid. Note, that only one layer of grid cells in the x_2 direction is laying inside a lens on the coarse grid.
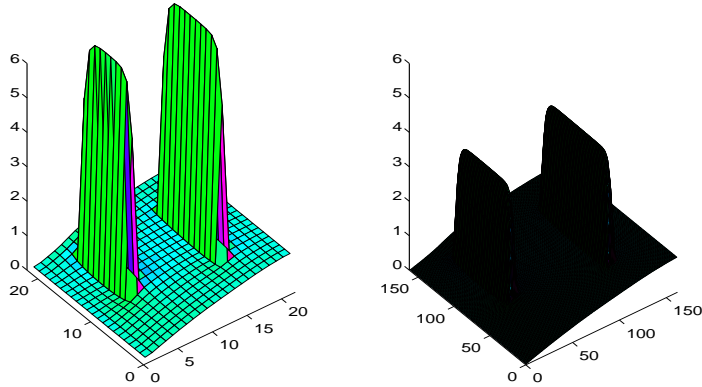
FIG. 4.2. *Graph of 2-D thin lenses computations with the HA scheme; left: grid* 22×22, *right: grid* 162×162
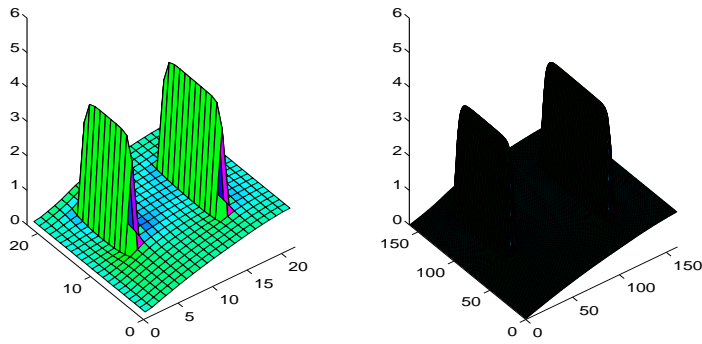

FIG. 4.3. *Graph of 2-D thin lenses computations with the IHA scheme; left: grid* 22×22, *right: grid* 162×162

The maximum values of the computed numerical solutions are presented in Table 4.9. In this case we refine the grid by tripling the number of nodes in any direction so we have nested grids, and we can monitor the value of the numerical solution at a fixed grid point on the plane.

Solutions, computed by IHA scheme are very close to the exact solution even when coarse grids are used (the first 3 digits of the maximum value of the solution are correct even on the coarsest grid). This fact is confirmed by the plots on Figure 4.2, as well as by the data in Table 4.9. At the same time, HA scheme produces rough approximation to the solution on the coarse grid. The AA scheme is practically unusable for coarse grids, and produces an inaccurate solution even on a very fine grid.

It should be noted, that in addition to the thin lenses problem, we have also computed the above example in the cases when the diffusion coefficient takes value

TABLE 4.9

2-D thin lenses problem; the maximum value of the numerical solution

Grid	A A	HA	IHA
22×22	1.0000	7.1186	3.9940
62×62	2.2620	4.3444	3.9952
182×182	3.3417	4.0356	3.9961
542×542	3.7970	4.0012	3.9965

TABLE 4.10

3-D problem with 8 subregions; the relative C-norm of the error

Grid	B	A A	HA	IHA
18^3	7.35d-5	2.05d-1	6.13d-3	8.43d-5
34^3	1.51d-5	1.13d-1	2.10d-3	1.62d-5
66^3	2.29d-6	5.90d-2	6.53d-4	3.71d-6

10^{-4} in larger domains (say, in an internal square which cover several grid nodes in each direction, etc.). In all cases IHA scheme produces much better results than HA scheme. However, IHA seems to be especially efficient for thin lenses problems. A possible explanation for this phenomenon is that in the case of thin lenses problems the solution behaves in some subregions as a function of one variable; therefore, the scheme reduces to a scheme for one-dimensional problem. As we know, for $f(x) \equiv 1$, this scheme is exact.

4.3. Numerical experiments for 3-D problems. We solved a 3-D problem (suggested in [6]) with non-homogeneous Dirichlet boundary conditions and known solution $u^{ex} = \frac{1}{k}(x_1 - 0.5)(x_2 - 0.5)(x_3 - 0.5) \ sin(\frac{\pi x_1}{2}) \ (1 + x_1^2 + x_2^2 + x_3^2)$, where k is a constant over each of the eight corners of this cube. More precisely, $k = \{10^2, 10^3, 10^7, 10^8, 10^{-2}, 10^{-1}, 10^3, 10^4\}$ in the eight corners, counting from the left to the right, and from the bottom to the top. Interfaces are aligned with the finite volume surfaces in this case, i.e. $\theta = 0.5$. The results from the numerical experiments are presented in Tables 4.10 and 4.11. In all cases we use the discretization of the boundary conditions reported in [8]. Table 4.10 and 4.11 show that the numerical solution of the interface problem, obtained with the new scheme (3.4), is at least two orders more accurate than the numerical solutions, computed with the other two schemes. Table 4.10 shows that the AA scheme does not provide a satisfactory accuracy, especially in the maximum norm. The HA scheme is much better, and the new IHA scheme produces the best results. We note that the solution computed with the new scheme on the coarsest grid with 18^3 points is more accurate than the solution computed by the HA scheme on the finest grid. The same observation can be made when comparing the arithmetic and harmonic averaging schemes. The HA scheme will need approximately 16^{11} nodes to produce the solution with the accuracy achieved by the new scheme on a 18^3-node grid. It can be also observed from Tables 4.10 and 4.11 that the constant of convergence of the new scheme does not depend on the jump of discontinuity in this example, and it is practically equal to the constant of convergence rate of the scheme for Poisson's equation.

5. Conclusions. A family of new difference schemes for self-adjoint second-order elliptic equations with discontinuous coefficients is derived via a finite volumes approach. A new scheme, based on improved harmonic averaging of the coefficient, has second-order accuracy under the following assumptions: (1) the diffusion coefficient matrix $K(x)$ is diagonal; (2) the interfaces are planes perpendicular to the coordinate axes; (3) the normal (to the boundaries of a given finite volume) component of the

TABLE 4.11
3-D problem with 8 subregions; the relative L_2-norm of the error

Grid	B	AA	HA	IHA
18^3	8.26d-6	1.01d-2	3.70d-4	9.40d-6
34^3	2.18d-6	4.59d-3	1.03d-4	1.86d-6
66^3	5.93d-7	2.19d-3	2.71d-5	4.31d-7

flux is continuously differentiable at the finite volume boundaries. Second-order convergence of the new scheme in the maximum-norm is observed in various numerical experiments for problems in R^n, $n = 1, 2, 3$. The numerical experiments also demonstrate that the new scheme is much more accurate than the known schemes in solving interface problems, especially in the cases of large jumps of the coefficient. The advantages of the new scheme are better seen in solving multidimensional problems with many interfaces and thin lenses problems.

ACKNOWLEDGMENTS.

REFERENCES

[1] O. Axelsson, V. Barker, *Finite Element Solution of Boundary Value Problems: Theory and Computations*, Academic Press Inc, 1984.

[2] Z.Q. Cai, On the finite volume element method, *Numer. Math.*, **58** (1991) 713-735.

[3] Z.Q. Cai, J. Mandel, and S. McCormick, The finite volume element method for diffusion equations on general triangulations, *SIAM J. Numer. Anal.* **38** (1991), 392–402.

[4] S.H. Chou and P.S. Vassilevski, A general mixed co-volume framework for constructing conservative schemes for elliptic problems, manuscript (1997), (to appear in *Math. Comp.*).

[5] R.S. Falk and J.E. Osborn, Remarks on mixed finite element methods for problems with rough coefficients, *Math. Comp.* **62** (1994), 1–19.

[6] R.E. Ewing, J. Shen and P.S. Vassilevski, Vectorizable preconditioners for mixed finite element solution of second-order elliptic problems, *Int. J. Comput. Math.*, **44** (1992), 313–327.

[7] J.M. Hyman and M. Shashkov, Adjoint Operators for the Natural Discretizations of the Divergence, Gradient and Curl on Logically Rectangular Grids, *Applied Numerical Mathematics*, **25** (1997), 413-442.

[8] O.P. Iliev, On second order accurate discretization of 3-D elliptic problems with discontinuous coefficients and its fast solution with pointwise multi-grid solver, Technical report No.3, Institute of Mathematics and Informatics, Bulgarian Acad. Sci., (1997) *submitted to IMA J. Numerical Analysis*.

[9] O.P. Iliev, A modified finite volumes approach for elliptic equations, to appear, *Comptes rendus de l'Academie bulgare des Sciences*, **51** (1998), No.3.

[10] V.P. Il'in, High order accurate finite volumes discretizations for Poisson equation, *Siberian Math. Journal*, **37**, (1996), No.1, 151–169, (in Russian).

[11] H. Jianguo and X. Shitong, On the finite volume element method for general self-adjoint elliptic problems, *SIAM J. Numer. Anal.*, **35** (1998), 1762-1774.

[12] V.A. Kondratiev, Boundary value problems for elliptic equations in domains with conical and angular points, *Trudy Mosk. Matemat. Obschestva*, **16** (1967), 209-292, (in Russian).

[13] R.H. Li and Z.Y. Chen, *The Generalized Difference Method for Differential Equations*, Jilin University Publishing House, 1994.

[14] R.J. LeVeque and Z. Li, Erratum: The immersed interface method for elliptic equations with discontinuous coefficients and singular sources, *SIAM J. Num. Anal.*, **32** (1995), 1704.

[15] G.I. Marchuk, *Methods of computational mathematics*, Moscow, Nauka, 1980.

[16] I.D. Mishev, Finite Volume Methods on Voronoi Meshes, *Numer. Meth. for PDEs*, **14** (1998), 193–212.

[17] A.A. Samarskii, *Theory of difference schemes*, Moscow, Nauka, 1977.

[18] A.A. Samarskii, V.B. Andreev, *Difference methods for elliptic equations*, Moscow, Nauka, 1976 (in Russian).

[19] A.A. Samarskii, R.D. Lazarov, V.L. Makarov, *Difference schemes for differential equations with generalized solutions*, Moscow, Visshaya Schkola, 1987 (in Russian).

[20] M. Shashkov, *Conservative finite-difference methods on general grids*, CRC Press, Boca Raton, Florida, 1996.

[21] G. Strang and G. Fix, *An analysis of finite element methods*, Prentice-Hall Inc, N.J., 1980.

[22] A.N. Tikhonov and A.A. Samarskii, Homogeneous finite difference schemes, *Zhurn. Vychisl. Mat. Mat. Fiz.*, **1** (1961), 5-63 (in Russian).

[23] A.N. Tikhonov and A.A. Samarskii, Homogeneous finite difference schemes of high accuracy on non-uniform grids, *Zhurn. Vychisl. Mat. Mat. Fiz.*, **1** (1961), 425-440 (in Russian).

[24] R.S. Varga, *Functional and Approximation Theory in Numerical Analysis*, CBMN Regional Conference Series in Applied Mathematics, SIAM, Philadelphia, 1971.

[25] P. Wesseling, *An Introduction to Multigrid Methods*, Wiley, N.Y., 1991.